This is a repository copy of *A practical evaluation of the performance of Al2O3-water, TiO2-water and CuO-water nanofluids for convective cooling*.

White Rose Research Online URL for this paper:
http://eprints.whiterose.ac.uk/131074/

Version: Accepted Version

A practical evaluation of the performance of Al₂O₃-water, TiO₂-water and CuO-water nanofluids for convective cooling

Fahad S. Alkasmoul[a,b]*, M. T. Al-Asadi[a], T.G. Myers[c], H. M. Thompson[a], and M. C. T. Wilson[a] *

[a] Institute of Thermofluids, School of Mechanical Engineering, University of Leeds, UK
[b] King Abdulaziz City for Science and Technology in Riyadh, Saudi Arabia
[c] Centre de Recerca Matemàtica, Campus de Bellaterra, Edifici C, 08193, Bellaterra, Barcelona, Spain

Abstract

The convective heat transfer, pressure drop and required pumping power for the turbulent flow of Al₂O₃-water, TiO₂-water and CuO-water nanofluids in a heated, horizontal tube with a constant heat flux are investigated experimentally. Results show that presenting nanofluid performance by the popular approach of plotting Nusselt number versus Reynolds number is misleading and can create the impression that nanofluids enhance heat transfer efficiency. This approach is shown to be problematic since both Nusselt number and Reynolds number are functions of nanofluid concentration. When results are presented in terms of actual heat transfer coefficient or tube temperature versus flow rate or pressure drop, adding nanoparticles to the water is shown to degrade heat transfer for all the nanofluids and under all conditions considered. Replacing water with nanofluid at the same flow rate reduces the convective heat transfer rate by reducing the operating Reynolds number of the system. Achieving a target temperature under a given heat load is shown to require significantly higher flow rates and pumping power when using nanofluids compared to water, and hence none of the nanofluids are found to offer any practical benefits.

Keywords: nanofluids, heat transfer, viscosity, alumina, titanium oxide, copper oxide.

_____

*Corresponding author, email: fkassmoul@kacst.edu.sa; m.wilson@leeds.ac.uk

Nomenclature

A	Inside surface area of the test section tube (m^2)
C_p	Specific heat (J/kg.K)
D	Diameter of the test section tube (m)
f	Friction factor
H	Heat transfer coefficient (W/m^2 ^{o}C)
L	Length of test section tube (m)
Re	Reynolds number
T	Temperature (°C)
$T_{s,in}$	Inside surface test section temperature (°C)
$T_{b,m}$	Average bulk temperature along the test section (°C)

$T_{b,in}$	Inlet bulk temperature of the test section fluid (°C)
$T_{b,out}$	Outlet bulk temperature of the test section fluid (°C)
$T_{s,out}$	Outside surface test section temperature (°C)
Nu	Nusselt number
P	Pressure (Pa)
Pr	Prandtl number
V	Average fluid velocity (m/s)

Greek letters

ϕ	Volume fraction of nanofluids
β	Ratio between the nanolayer thickness surrounding the nanoparticle and the nanoparticle radius
ν	Kinematic viscosity (m^2/s)
ρ	Density (kg/m^3)
μ	Dynamic viscosity (Pa s)

Subscripts

av	Average
bf	Base fluid
nf	Nanofluid
p	Nanoparticle

1. Introduction

Nanofluids have proved beneficial in a wide range of applications, such as in the chemical, electrical and nuclear industries, in cancer diagnosis, solar energy capture, high-powered lasers, drilling and in enhanced oil recovery [1-4]. They have also been widely promoted for heat transfer applications, where it has been claimed that they can offer significantly enhanced heat transfer [5-7], while alleviating the problems of clogging, erosion and sedimentation associated with suspensions that contain larger particles [8]. Despite much theoretical and experimental promise for energy-related problems there is still a need to transfer the research into a practical reality. Specifically this means increasing the convective heat transfer in a manner which outweighs the accompanying increase in viscous pressure drop [9]. The present study evaluates the performance of nanofluid coolants from this practical perspective.

The intense interest in the potential use of nanofluids in heat transfer applications has resulted in the thermal and hydraulic properties of nanofluids being widely investigated. Many previous studies have reported anomalous increases in thermal conductivity not predicted by the classical Maxwell model. Wu & Zhao [9] refer to a spectacular improvement in thermal conductivity. Sergis & Hardalupas [10] carried out a statistical analysis of nanofluid data and found enhancements of thermal conductivity

typically between 1-24% (accounting for 45% of the data analysed) while 25% of the data indicated an enhancement over 29%, with some over 84%. This type of spread led to the proposal of new models and mechanisms, such as adaptations for non-spherical particles, surface layers and particle clustering, [11-13]. Motivated by the uncertainty surrounding nanofluid properties, Buongiorno et al. [8] carried out the International Nanofluid Property Benchmark Exercise (INPBE) in which the thermal conductivities of nanofluids were measured by 34 organisations worldwide. A diverse range of nanofluids were investigated, including aqueous/non-aqueous base fluids, metallic and metal-oxide particles, near spherical and elongated particles and low-to-high particle concentrations. In contrast to previous studies the INPBE concluded that the conductivity could be well-modelled by standard effective medium theory. In fact the Maxwell model is based on an assumption that a single particle lies in an infinite medium, consequently as particle concentrations increase it becomes less accurate. Myers et al. [14] showed that a standard analysis of heat flow over a finite region can lead to a better agreement with data for higher volume fractions, but again this is without resorting to exotic physical mechanisms.

In heat removal the goal is generally to achieve the required rate of cooling with a minimal power consumption. Since the latter depends on the nanofluid viscosity a number of studies have focussed on the viscous response of nanofluids. The Mahbubul et al. [15] investigation, for example, carried out a thorough review of studies into the viscosity of nanofluids and considered the effect of nanofluid preparation methods, temperature, particle size and shape and concentration on nanofluid viscosity. They found that concentration, particle shape and temperature all have significant effects on viscosity, whereas Azmi et al. [16] found that particle size was more influential than shape. In contrast to these studies, Sundar et al. [17] also found that the nanofluid preparation was also very influential. More recently, Bashirnezhod et al. [18], have considered that the existing experimental data on the thermophysical properties of nanofluids is neither sufficient nor reliable. They concluded that there is a pressing need for experimental studies which account for all the important factors including temperature, nanofluid concentration, nanoparticle size, pH, sonication time, aggregation and base liquid type to provide more accurate correlations for viscosity. They appear not to have been aware of the contemporaneous study of Meybodi et al. [2], who compiled an extensive database for water-based Al_2O_3, TiO_2, SiO_2 and CuO nanofluids and presented a formula to predict viscosity. They claim previous models have low accuracy while theirs, which involves only concentration, particle size and temperature, is superior.

The disagreements highlighted above have carried through to the primary goal of the research, namely the heat transfer performance. Many studies, both experimental and theoretical, claim that the addition of nanoparticles can lead to significant improvements in heat transfer performance compared to base fluids [2, 16, 19]. Fotukan & Esfahany [20] reported an average 25% increase in heat transfer coefficient and a simultaneous 20% reduction in pressure drop for very dilute CuO/water nanofluids. The statistical investigation of Sergis & Hardalupas [10] states that 19% of the papers studied showed an improvement

in convective heat transfer between 10 and 18%, while 11% of papers show a deterioration (the remaining papers indicated unspecified enhancement). Haddad et al. [19] carried out a numerical study and stated explicitly that the presence of nanoparticles always leads to an enhancement in heat transfer. However, a paper by the same group, in the same year (Haddad et al. [21]), states that while numerical results mostly indicate an enhancement experimental studies show that nanoparticles lead to a deterioration in heat transfer.

Haghighi et al. [22] have recently considered the practical benefits of nanofluids by investigating the advantages of Al_2O_3, TiO_2, SiO_2 and CeO_2 on thermo-physical properties and heat transfer coefficient. They noted that the benefits reported in the literature may be due to their representation in terms of Nusselt number versus Reynolds number, which can be misleading because both are strong functions of the nanoparticle concentration. Also, since the viscosity of nanofluids increases with nanoparticle concentration, the flow rate must be increased to provide the same Reynolds number. As convective heat transfer rate increases with flow rate it is not appropriate to compare the performance of the base fluid (less viscous) with the nanofluid (more viscous) at the same Reynolds number. They proposed that it is more meaningful to compare the heat transfer rate for a given pumping power. When they did this, they found that the nanofluid performance was actually worse than water. The errors caused by comparison using non-dimensional parameters is discussed in greater detail in Myers et al. [23]: as stated above it does not make sense to compare Reynolds numbers which are scaled with concentration dependent properties, neither Nusselt numbers which are scaled with thermal conductivity. The authors continue with a critique of mathematical studies highlighting common errors, such as incorrect governing equations and parameter values that lead to the enhancements predicted by these theoretical studies.

Despite the wealth of literature concerning nanofluid properties and performance there remain many inconsistencies and much confusion, and consequently the current body of data is neither sufficient nor reliable for engineering applications. The purpose of the present study is to present results for the heat transfer properties and performance of standard nanofluids and to clarify a number of issues arising from previous studies. Specifically we undertake a comprehensive experimental evaluation of the heat transfer, pressure drop and power consumption for Al_2O_3, TiO_2 and CuO-water nanofluids for cooling applications. In the following section the nanofluid preparation methods are outlined. In section 3 the experimental configuration and measurement techniques are described, and their validation against the literature is presented in section 4. The experimental results are given in section 5, together with comparisons against previous work and an assessment of the nanofluid performance from a practical perspective. Conclusions are summarised in section 6.

2. Nanofluid preparation and morphology

Many types of nanofluids are available that differ with regard to host liquid types, such as water, ethylene glycol or oil, as well as the nanoparticle material, volume concentration, particle size and shape

[4, 7, 24]. In the present study, aqueous aluminium oxide (Al$_2$O$_3$-water), titanium oxide (TiO$_2$-water) and copper oxide (CuO-water) nanofluids were chosen because they are the most commonly used by researchers and so are easily comparable. They are commercially available and simple to prepare.

The aluminium oxide (Al$_2$O$_3$-water) nanofluid was prepared by using a two-step technique. The nanoparticles were supplied by Sigma-Aldrich, with an average size of 50 nm, and added to de-ionized water using magnetic stirring and ultrasonic agitation to disperse the particles in the base fluid to obtain a nanofluid with mass fraction 20 wt.%. Titanium oxide (TiO$_2$-water) and copper oxide (CuO-water) nanofluids were purchased from Alfa Aesar as colloidal dispersion nanofluids with mass fraction 50 wt.% and particle size 45 nm (TiO$_2$) and 35 wt.% and 30 nm (CuO). These concentrations of the nanofluids were diluted with de-ionized water to create nanofluids with a variety of volume fractions in the ranges 0.5-3.6 vol% (Al$_2$O$_3$), 0.5-4.5 vol.% (TiO$_2$) and 0.4-1.6 vol.% (CuO).

The nanoparticle morphologies of the synthesized and purchased nanofluids were verified using Transmission Electron Microscopy (TEM), Jeol JEM-2100F model, as shown in Figure 1. The images show that Al$_2$O$_3$ and TiO$_2$ nanoparticles are non-spherical, irregular shapes with a variety of sizes; the average size of the particles is about 50 nm and 45 nm respectively. In contrast, the CuO nanoparticle is almost spherical with an average typical diameter of 30 nm (as stated by the manufacturer). The TEM was used to determine the particle size and shape as well as the agglomeration of nanoparticles. As observed in Figure 1, the nanoparticles aggregate forming larger particles. However, the drawback of the TEM is that the sample of nanofluid should be dried out before being inserted inside the device, and this causes agglomeration of the nanoparticles. Hence the agglomeration observed in Figure 1 could result either from the drying process or in the original sample itself.

The thermal and physical properties of water and the nanoparticles were calculated from the existing literature and these properties were used to determine the nanofluid properties, except for the viscosity, which was measured directly. The properties of water were taken from Abbasian and Amani [25] with an uncertainty of about 1.3% and the properties of Al$_2$O$_3$, TiO$_2$ and CuO nanoparticles at room temperature were taken from the literature and are summarized in Table 1.

The nanofluid density, ρ_{nf}, and specific heat capacity, $C_{p,nf}$, are taken from the equation of mixture theory and thermal equilibrium, as this gives good agreement with the experimental results of Pak & Cho [26], Heyhat et al. [27], Mondragon et al. [28], Khanafer & Vafai [29] and Utomo et al. [30]. Hence:

$$\rho_{nf} = \rho_{bf}(1-\phi) + \rho_p\phi \tag{1}$$

$$(\rho C_p)_{nf} = (\rho C_p)_{bf}(1-\phi) + \phi(\rho C_p)_p \tag{2}$$

where ϕ is the volume fraction and ρ_p and $C_{p,p}$ are respectively the density and specific heat capacity of the nanoparticles.

As discussed above, the thermal conductivity of nanofluids, k_{nf}, can be calculated by physically consistent approaches such as the classical Maxwell model and the recent model by Myers et al. [14]. Table 2 compares the predicted values of k_{nf} from these two models for Al_2O_3/water nanofluids against the predictions from Yu and Choi's model [12]. The latter has been shown to agree well with thermal conductivity experiments for a range of different nanofluids by Williams et al. [31], Heyhat et al. [27], Mondragon et al. [28] and Duangthongsuk & Wongwises [32]. The agreement between all three models is very good. All the results reported below have calculated k_{nf} using the model of Myers et al. [14].

Since the viscosity of the nanofluids determines the required pumping power, it was obtained directly from laboratory measurements. It is noted that the viscosity of nanofluids varies according to type of nanoparticles and depends on many other factors such as nanoparticle concentration and temperature. The following equations were created to fit the experimental data, and subsequently used in the convective heat transfer calculation:

$$\frac{(\mu_{nf})_{Al_2O_3}}{\mu_{bf}(T)} = \exp(6.599\phi/(0.288-\phi)) \qquad \text{for } \phi = 0 \text{ to } 4.0 \text{ vol.\%, } R^2 = 0.9973 \qquad (4)$$

$$\frac{(\mu_{nf})_{TiO_2}}{\mu_{bf}(T)} = 25.17\phi^2 + 29.562\phi + 1 \qquad \text{for } \phi = 0 \text{ to } 4.5 \text{ vol.\%, } R^2 = 0.9977 \qquad (5)$$

$$\frac{(\mu_{nf})_{CuO}}{\mu_{bf}(T)} = 776.28\phi^2 + 7.7392\phi + 1 \qquad \text{for } \phi = 0 \text{ to } 2.0 \text{ vol.\%, } R^2 = 0.9963 \qquad (6)$$

Here μ_{nf} and μ_{bf} refer to the viscosities of the nanofluid and base fluid respectively, and T is the temperature. Figure 2 plots the experimental data relative viscosities captured by Eqs. (4)-(6).

3. Measurement Techniques and Experimental Methodology

This study uses a forced convective heat transfer experimental technique to evaluate the thermal characteristics and pressure drop of the nanofluids. The convection loop setup is shown in Figure 3. The loop includes two test sections, namely the heated test section and the isothermal test section, with both sections consisting of a hollow circular tube of stainless steel (seamless stainless steel (SS) 316 / 316L based on ASTM standards) with outer and inner diameter and length of 0.5in (0.0127 m), 0.37in (0.0094 m) and 121.6in (3.040 m), respectively. The pump (1 HP stainless steel STA-RITE pump) is used to circulate the fluids through the loop. The flow rate is determined by a turbine flow meter (FTB-902, OMEGA), with accuracy 0.5% within the flow range 0.75 to 5 GPM, and pressures are measured using differential pressure transducers (OMEGA PX293- 030D5V with operating range 0 to 207 kPa (0 to 30 psid) and accuracy within 0.5%) and gauge pressure transducers. The DC power supply (GENESYS 10 kW (20 V and 500 A), TDK-Lambda Americas Inc) generates heat uniformly within

the body of the heated test-section and before and after the test section. The fluid bulk temperature and pressure drop is measured using the submerged thermocouples and differential pressure transducers. The outer surface temperature of the test section is also measured using 14 T-type thermocouples (T-type thermocouples (TJC36-CPSS-032U-12, OMEGA); accuracy of 0.5 °C or 0.4% from 0 – 350 °C) attached along the test section top outer surface. These procedures enable detailed measurement of the temperature variation over the top surface of the heated test section. The heat exchanger is used to remove the heat and control the inlet test section temperature. The temperature and pressure before and after the unheated test section are also measured by submerged thermocouples and differential pressure transducers, before the fluid returns to the accumulator tank where the cycle starts again. In order to control the flow rate of the loop, a by-pass valve to the accumulator tank is included. All data was acquired and recorded using National Instruments' data acquisition device and LabView software.

3.1 Heat Transfer Measurement

The purpose of the experimental technique is to evaluate the convective heat transfer coefficient from the measurable quantities by applying the relevant equations. The heat transfer coefficient, h, represents the rate of heat transferring per unit area through the solid surface into the fluid as a result of a temperature difference between the solid and the fluid flowing over it:

$$q'' = h\Delta T$$

where q'' is the heat flux through the solid-fluid boundary and ΔT is the temperature difference between the boundary fluid near the solid surface and the far field fluid. The interpretation of this ΔT varies [33], but commonly it is assumed that the temperature near the solid surface is the same as the temperature of the surface [34]. The temperature of the far field fluid is the average temperature between the inlet and outlet tube [33]. This assumption is used in this study to give $\Delta T = T_{s,in} - T_{b,m}$ and then the heat transfer coefficient is:

$$h = \frac{q}{A(T_{s,in} - T_{b,m})} \tag{7}$$

where q is heat input to the test section, A is the inside surface area of the test section (calculated from $A = \pi D_{in} L$, where D_{in} (m) is the test section diameter and L(m) the test section length), $T_{s,in}$ is the inside surface test section temperature and $T_{b,m}$ is the average bulk temperature along the test, [26], [31], [35]:

$$T_{b,m} = \frac{T_{b,in} + T_{b,out}}{2} \tag{8}$$

where $T_{b,in}$ and $T_{b,out}$ are respectively the inlet and outlet bulk temperatures of the test section fluid, measured by the submerged thermocouples. Note that the thermo-physical properties of the fluids (water and nanofluid) are taken at the average bulk temperature, $T_{b,m}$.

The Nusselt number is defined as [35]:

$$Nu = \frac{hD}{k} \tag{9}$$

where D is the diameter of the test section and k is the thermal conductivity of the fluid.

3.2 Measurement procedure

Measurements were carried out for one specimen of each concentration for each nanofluid. This was repeated three times for each specimen and then the mean values of the results were obtained. The inlet bulk temperature of the test section was maintained at around 20 °C and their form heat generation at about 5000W and the flow rate was changed from 0.75 to 2.0 GPM (US gallons per minute – i.e. 5×10^{-5} to 0.00013 m^3/s) for each sample. This process was run initially with water and then the nanofluids to provide similar conditions for comparison. The loop system was considered to be steady state under constant inlet temperature and constant heat flux. After the tests reached a steady state condition, the temperature, pressure and flow rate data was recorded for each three-minute duration at a rate of two data recordings per second. This was repeated three times for each sample and then mean values of these data were obtained by averaging.

In order to implement nanofluids in the loop with desired concentrations, it is necessary to load the loop with the highest nanofluid concentration first and then dilute to the lower concentrations.

4. Experimental Verification

Before exploring the performance of the nanofluids, the heat transfer and pressure drop characteristics of water were first measured to verify the reliability of the experimental system (loop). Water properties and performance are well known in the literature [25], [36].

4.1 Heat transfer verification test for water

The experimental methods were validated by comparison with Gnielinski's correlation [36]:

$$Nu_{ave} = \frac{(f/8)(Re-1000)Pr}{1+12.7(f/8)^{1/2}(Pr^{2/3}-1)} \tag{10}$$

for $0.5 \leq Pr \leq 2000$ and $3000 \leq Re \leq 5 \times 10^6$, where f is the friction factor obtained by the Petukhov relation [36] as:

$$f = (0.790 \ln Re - 1.64)^{-2}. \tag{11}$$

Here Re is the Reynolds number and Pr the Prandtl number, defined as:

$$Re = \frac{\rho VD}{\mu} \quad , \quad Pr = \frac{C_p \mu}{k}$$

where ρ, μ, k, C_p are respectively the density, dynamic viscosity, thermal conductivity and specific heat of the fluid, V is the average fluid velocity and D is the diameter of a tube. The validation was carried out by using water with a range of Reynolds numbers from 8900 to 19500.

Figure 4 shows a comparison of the measured average Nusselt number of water (Nu_{ave}) to the predicted Nusselt number by using Gnielinski's correlation. In order to facilitate comparison, the error +/-5% of the measured result and the predicted results are presented as dotted lines. It can be seen that the data of average Nusselt number falls within 5% of the predicted values. This indicated that the experimental loop is reliable for measuring the turbulent heat transfer coefficient. The experimental uncertainty of the measured Nusselt numbers is estimated to be ±5%.

4.2 Pressure drop verification test for water

The measured pressure drop (ΔP) of the loop using water was compared with the existing correlation of fully developed turbulent flow, assuming the surface of the tube to be smooth [36]:

$$\Delta P = f\ \frac{L}{D}\left(\frac{\rho V^2}{2}\right) \tag{12}$$

where L and D are respectively the length and inner diameter of the test section tube. The friction factor, f, can be calculated from Eq. (11). The pressure drop measurement results for the heated test section and isothermal test were in close agreement with the conventional semi-theoretical Eq. (12) as shown in Figure 5, with a difference of less than 10%. The average experimental uncertainty of the measured pressure drop is estimated to be ±7%.

From the above heat transfer and pressure drop tests, it can be concluded that the experimental set-up is reliable for measuring the heat transfer and the pressure drop of turbulent liquid flow. Next, measurements of the convective heat transfer and pressure drop for the nanofluids will be described.

5. Results and discussion

This section presents the convective heat transfer performance and pressure drop for the nanofluids under consideration as a function of the volumetric concentration of nanoparticles.

5.1 Heat transfer characteristics of nanofluids

The convective heat transfer coefficient (h_{ave}) and pressure drop for all nanofluids (Al_2O_3-water, TiO_2-water nanofluid and CuO-water) with various nanoparticle concentrations were measured and compared to the base fluid (water). In previous studies, a popular approach in assessing the thermal performance of nanofluids is to consider the variation of the Nusselt number with the Reynolds number. Adopting this approach, for now, using the data from the present study, leads to the plots in Figure 6 for the three types of nanofluid considered. Note that Nu and Re are determined using the nanofluid properties taken

at the bulk mean temperature. In each plot, the performance of the water base fluid is given for comparison. For TiO_2 nanofluids, the nanoparticle loading has no distinguishable effect on the value or variation of the average Nusselt number with Reynolds number. For CuO nanofluids, the nanoparticle loading has more influence, with lower concentrations giving slightly lower values of Nusselt number at a given Reynolds number, but with 1.2% and 1.6% concentrations giving slightly higher Nusselt numbers. In contrast, for the Al_2O_3 nanofluids the nanoparticle loading has a marked effect on the behaviour, with the average Nusselt number increasing with nanoparticle load for a given Reynolds number. For example, at a Reynolds number of about 8000 the Nusselt number increased by 7%, 10% 22%, 39%, and 54% for Al_2O_3-water nanofluids with loading 0.5, 0.9, 1.8, 2.7 and 3.6 vol.% respectively.

These plots suggest that using Al_2O_3-water nanofluids would be beneficial and lead to an enhanced heat transfer rate. However, they are misleading because both Nu and Re are themselves dependent on the nanoparticle loading, ϕ. The Nusselt number is scaled with thermal conductivity, which is a function of ϕ, while Re includes the density and viscosity and both these properties also depend on the nanoparticle concentration. Moreover, the viscosity of each nanofluid is higher than the base fluid, and increases with increasing nanoparticle concentration, so each nanofluid requires a higher flow rate in order to achieve the same corresponding Reynolds number as the base fluid.

To reveal the true effect of using nanofluids, the actual (dimensional) heat transfer coefficient should be considered, as a function of the (dimensional) flow rate. This leads to Figure 7, which gives representative results of the variation of the average heat transfer coefficient with volumetric flow rate and different volume concentrations of Al_2O_3-water nanofluid, TiO_2-water nanofluid and CuO-water nanofluid, respectively. The corresponding curves for the base fluid (distilled water) are presented as solid lines.

It is now clear that the water itself actually outperforms all of the nanofluids considered – it has the highest heat transfer coefficient under the experimental conditions. In other words, nanofluids have a deleterious effect on convective heat transfer and this deterioration increases with increasing nanoparticle load. For example, the convective heat transfer coefficient decreases noticeably with Al_2O_3-water nanofluid concentrations of $0.5 - 3.6$ vol.% leading to reductions of between 5 to 25%, respectively. Whereas, TiO_2-water nanofluids with volume fraction 0.5, 1.5, 2.5, 3.5 and 4.5 vol.% give respective decreases in heat transfer coefficient of 11%, 24%, 34%, 43% and 50% compared to the base fluid. For CuO-water nanofluids, at given volumetric flow rate, the base fluid has the highest heat transfer coefficient by an average of 8%. Note that only low concentrations of CuO-water nanofluid were investigated, due to their high cost. The trend observed in Figures 6 and 7, showing a decrease in heat transfer with increasing particle concentration, was predicted theoretically in MacDevette et al. [33] by applying standard boundary layer theory.

The heat transfer performance of the nanofluids is actually even worse than indicated in Figure 7 when one considers the pressure drop in the system. As the nanoparticle concentration increases, the viscosity of the nanofluid increases, and therefore the pressure gradient required to achieve a certain flow rate also increases. Hence if the heat transfer coefficient at fixed pressure gradient were considered, the reduction in heat transfer coefficient with increasing nanoparticle concentration would be even greater. In order to achieve the same Reynolds number as the pure base fluid a much greater pumping power is required. This is discussed further in Section 5.5.

5.2 Comparison with previous experimental results

Sahin et al. [39] measured the heat transfer coefficient in a similar experimental set-up using Al_2O_3-water nanofluids with similar volume fraction to those considered here. Figure 5 of their paper presents their measured heat transfer coefficient as a function of Reynolds number, and Figure 8 of the present work replots their data in terms of volumetric flow rate. The flow rate was determined from the Reynolds number using the nanofluid viscosity and density data given in Table 2 of Ref. [39], together with the stated dimensions of the pipe. For comparison, Figure 8 also shows our Al_2O_3 data from Figure 7. Note that, apart from the 0.5% case, the volume fractions are slightly different in the two studies.

As can be seen in Figure 8, there is generally good agreement in the measured heat transfer coefficient, particularly at lower flow rate and lower volume fraction. It is not clear what size of nanoparticles were used in the nanofluids studied by Sahin et al. [39], however the discrepancy in reported viscosities of the corresponding nanofluids suggests there are some constitutive differences in the nanofluids that could account for the difference in heat transfer performance at higher flow rates and volume fractions. Nevertheless, when plotted against flow rate, the data of Sahin et al. [39] also show that the heat transfer performance is reduced as the nanoparticle loading is increased. Pak and Cho [26] also noted that under the condition of constant average flow speed, and hence constant flow rate, the convective heat transfer coefficient of their Al_2O_3 nanofluid was 12% lower than that of pure water. This is considered further in Section 5.5.

Pak and Cho [26], Sahin et al. [39] and Sajadi and Kazemi [35] all report experimental investigations of nanofluid performance in which all the resulting measurements are captured in the form of (different) correlations giving the Nusselt number in terms of Reynolds number and Prandtl number (Pr). These correlations provide a means of comparing our observations with a wider collection of previous experiments. Pak and Cho [26] established their correlation,

$$\mathrm{Nu_{Pak}} = 0.021 \mathrm{Re}^{0.8} \mathrm{Pr}^{0.5} \tag{13}$$

based on their experimental data for γ-Al_2O_3-water and TiO_2-water nanofluids with $0 \le \phi \le 3$ vol.%, $10^4 \le \mathrm{Re} \le 10^5$ and $6.54 \le \mathrm{Pr} \le 12.33$. The correlation

$$\mathrm{Nu_{Sahin}} = 0.106 \mathrm{Re}^{0.588} (1.0 + \phi^{0.1096}) \mathrm{Pr}^{0.258} \tag{14}$$

was constructed by Sahin et al. [39] from their experimental data on Al_2O_3-water nanofluids with $0.5 \le \phi \le 4$ vol.%, $4 \times 10^3 \le Re \le 2 \times 10^4$ and $6 \le Pr \le 7$. Sajadi and Kazemi [35] derived their correlation,

$$Nu_{Sajadi} = 0.067 \, Re^{0.71} \, Pr^{0.35} + 0.0005 \, Re \qquad (15)$$

from their data on TiO_2-water nanofluids with $0 \le \phi \le 0.25$ vol.% and $5 \times 10^3 \le Re \le 3 \times 10^4$.

Figure 9(a) shows a comparison of the average Nusselt numbers measured from all our Al_2O_3 experiments with the Nusselt numbers predicted by correlations (13) and (14) using the corresponding nanofluid properties (taken at the average bulk temperature) and flow rates for each experiment to determine the parameters in the equations. The Pak and Cho [26] correlation, eq. (13), predicts values very close to those observed – the difference is within 5%. It should be noted that the experimental uncertainty in the measured Nusselt numbers are estimated to be ± 3 to 9%. On the other hand, the Sahin et al. [39] correlation (14) gives a noticeable over-prediction of Nu. This is probably because the Prandtl number in our experiments is higher than in [39], since the measured viscosity of the Al_2O_3-water nanofluid is higher. For example $Pr = 11$ at $\phi = 3.6$ vol.%.

For the TiO_2-water nanofluids, Figure 9(b) shows a comparison of our experimentally determined average Nusselt numbers with the values predicted by correlations (13) and (15) again with the parameters in the expressions determined from the corresponding nanofluid properties and flow conditions for each experiment. Though there is still good agreement with eq. (13) for some conditions, there is more scatter and for some conditions eq. (13) over-predicts the corresponding Nu by up to 20%. The Sajadi and Kazemi [35] correlation (15) also over-predicts Nu compared to our experiments. The discrepancy is less than 20% at high Re, but at low Re there is a substantial over-prediction of more than 40%. This is possibly because they used Einstein's model to predict the viscosity of nanofluids for the correlation and this theoretical viscosity model significantly underestimates the nanofluid viscosity.

5.3 Comparison with the Gnielinski correlation

The correlations (13)-(15) are all developed specifically for nanofluids. The measured average Nusselt number values from our nanofluid experiments were also compared with the predictions of Gnielinski's well-known correlation, Eq. (10), to explore how well it can estimate the Nusselt number if the nanofluid properties are used in Re and Pr. The comparison is shown in Figure 10. It is found that the predicted Nu_{ave} for CuO-water nanofluid agrees well to within 10% of the experimental value. The measured Nusselt number values for Al_2O_3-water and TiO_2-water nanofluids at low volume fraction ($\le$ 1.8 vol.% and $\le$ 2.5 vol.% respectively) are within about 10% of Gnielinski's correlation; however, a difference of nearly 20% was found for higher volume fractions, particularly for TiO_2-water. It is interesting to note that the Gnielinski correlation underestimates the average Nusselt number for the Al_2O_3-water nanofluid but mostly over-predicts it for the TiO_2-water nanofluid. Alkasmoul [37]

estimated that the experimental uncertainty of the measured Nusselt numbers for Gnielinski's correlation and nanofluids are $\pm$ 10% and 3-9%, respectively.

5.4 Pressure drop

Figure 11 shows that the theoretical correlation Eq. (12) predicts well the pressure drop observed in the system across all nanofluids and operating conditions considered. Almost all data lie within the $\pm$10% interval shown by the dashed lines in figure 11.

The pressure drop measured for all nanofluids over a range of Reynolds number is plotted in figure 12. The pressure drop for each fluid increases with Reynolds number, as is to be expected, but at a rate that increases significantly with increasing nanoparticle loading. The highest value of the viscous pressure losses is observed for the nanofluids with the largest volume fraction, and this is mainly because the viscosity increases with nanoparticle load.

5.5 Assessment of the nanofluids as coolants

The dimensionless correlations discussed above provide a means of condensing many observations to represent complex behaviour in a functional form. However, for a practical evaluation of the nanofluids, as is the goal of this paper, the correlations by themselves are not sufficient. In practical cooling applications, key concerns are: (i) whether or not the system can be maintained below a critical temperature under a given heat load, (ii) for what conditions this can be achieved, and (iii) what is the associated energy cost in creating those conditions. To examine the performance of the nanofluids from this practical perspective, figure 13 shows how the outside surface temperature of the heated test section varies with flow rate for different concentrations of the three nanofluids. The figure also includes corresponding plots using the associated pressure drop rather than flow rate, as it directly relates to the associated pumping costs.

Once again, observing the nanofluid performance in terms of dimensional quantities highlights that none of the nanofluids offers any improvement in heat transfer performance compared to the distilled water base fluid (data shown as a dashed line). At a given flow rate or pressure drop, increasing the loading of the nanoparticles in the nanofluid results in a higher surface temperature – significantly so in the case of Al_2O_3 and TiO_2 nanofluids. More importantly, from the practical perspective, this means that achieving a given surface temperature using a nanofluid rather than water requires a higher flow rate – in some cases almost double the flow rate. For example, to achieve an outside surface temperature of 45°C with water requires a flow rate of around 1.5 GPM but with the addition of 4.5% TiO_2 particles the flow rate must be increased to around 2.8 GPM. Furthermore, achieving that surface temperature with water as the coolant involves a pressure drop of about 33 mbar, but with 4.5% TiO_2 the pressure drop increases to about 110 mbar. Since the pumping power required is the product of the pressure drop and the volumetric flow rate, using this nanofluid to achieve the 45°C temperature would require over six times more pumping power than using water.

Similar observations can be made for the Al_2O_3-water nanofluids, and these are perhaps more telling, since the dimensionless Nu-Re plots of Figure 6 at first glance suggest that the Al_2O_3-water nanofluids offer significantly higher heat transfer rates. In fact, Figure 13 shows that achieving the same example target temperature of 45°C with the 3.6% Al_2O_3-water nanofluid would require a flow rate of about 2.25 GPM with a corresponding pressure drop of 72 mbar, resulting in a pumping power three times greater than that required for water.

All the nanofluids considered in the present study were found to be less effective and less efficient than water. The key problem with these nanofluids is that the increase in both the dynamic and kinematic viscosities with nanoparticle concentration outweighs any gain in thermal conductivity. For a fixed volumetric flow rate of coolant, and hence fixed average flow velocity, the higher kinematic viscosity means that the corresponding Reynolds number for the nanofluid flow is lower than that of water at the same speed. It is well known, as all of the correlations above show, that the convective heat transfer rate increases with Reynolds number. Hence replacing water with a nanofluid driven at the same flow rate reduces the heat transfer rate as a result of reducing the operating Reynolds number of the system. An increase in flow rate and pumping power would be required to achieve the same performance as water, so there is no benefit to be gained in using any of the considered nanofluids.

6. Conclusion

This study explores the heat transfer performance of the common nanofluids Al_2O_3-water, TiO_2-water and CuO-water, from a practical perspective. The experimental technique was set up for forced convection within the turbulent regime, and used to measure and evaluate the heat transfer characteristics and pressure drop of nanofluids under turbulent flow conditions. The results show that:

- At any specific flow rate, the heat transfer rate achieved with the base fluid alone was better than that of all the nanofluids considered. This means that using nanofluids at fixed flow rate degrades the heat transfer rate compared to the base fluid, and this deterioration increases with increasing nanoparticle load. As a result, significantly higher surface temperatures are observed when using nanofluids, and substantially higher flow rates and pumping costs are required to maintain a given surface temperature using a nanofluid compared to water.

- Assessing the thermal performance of nanofluids by considering the Nusselt number and its variation with Reynolds number is misleading because both Nusselt number and Reynolds number depend on the nanofluid properties (i.e. thermal conductivity, density and viscosity that are functions of the nanoparticle volume fraction). This can lead to a false conclusion that some nanofluids produce an improvement in heat transfer performance.

- The pressure drop using nanofluids increases significantly with increasing flow rate and nanofluid concentration, since the nanofluid viscosity increases substantially with increasing nanoparticle load.

- Replacing water with a nanofluid at the same flow rate would reduce the operating Reynolds number of the system because of the increase in kinematic viscosity, leading to a reduction in convective heat transfer rate. Achieving the same performance as water would require an increase in flow rate and several times more pumping power than required for water.

- The heat transfer coefficient and pressure drop expected for the nanofluids can be predicted very well using the existing conventional correlation for a single phase fluid, if the properties of the nanofluid are used. This has been noted previously, e.g. by Williams et al. [31] and Heyhat et al. [27].

From the above, it is concluded that the nanofluids tested here do not offer any practical benefits in terms of enhanced heat transfer performance.

References

[1] R. Saidur, K. Y. Leong, and H. A. Mohammad, "A review on applications and challenges of nanofluids," Renewable and Sustainable Energy Reviews, vol. 15, pp. 1646-1668, 2011.

[2] M. K. Meybodi, A. Daryasafar, M. M. Koochi, J. Moghadasi, R. B. Meybodi, and A. K. Ghahfarokhi, "A novel correlation approach for viscosity prediction of water based nanofluids of Al_2O_3, TiO_2, SiO_2 and CuO," Journal of the Taiwan Institute of Chemical Engineers, vol. 58, pp. 19-27, 2016.

[3] A. S. Kherbeet, M. R. Safaei, H. A. Mohammed, B. H. Salman, H. E. Ahmed, O. A. Alawi, et al., "Heat transfer and fluid flow over microscale backward and forward facing step: A review," International Communications in Heat and Mass Transfer, vol. 76, pp. 237-244, 2016.

[4] M. Al-Asadi, H. Mohammed, S. Akhtar, A. S. Kherbeet, and H. Dawood, "Heat Transfer Enhancements Using Traditional Fluids and Nanofluids in Pipes with Different Orientations: A Review," Journal of Nanofluids, vol. 6, pp. 987-1007, 2017.

[5] J. Albadr, S. Tayal, and M. Alasadi, "Heat transfer through heat exchanger using Al2O3 nanofluid at different concentrations," Case Studies in Thermal Engineering, vol. 1, pp. 38-44, 2013.

[6] A. S. Kherbeet, H. A. Mohammed, H. E. Ahmed, B. H. Salman, O. A. Alawi, M. R. Safaei, et al., "Mixed convection nanofluid flow over microscale forward-facing step — Effect of inclination and step heights," International Communications in Heat and Mass Transfer, vol. 78, pp. 145-154, 2016.

[7] M. T. Al-asadi, H. A. Mohammed, A. S. Kherbeet, and A. A. Al-aswadi, "Numerical study of assisting and opposing mixed convective nanofluid flows in an inclined circular pipe," International Communications in Heat and Mass Transfer, vol. 85, pp. 81-91, 2017.

[8] J. Buongiorno, D. C. Venerus, N. Prabhat, T. McKrell, J. Townsend, R. Christianson, et al., "A benchmark study on the thermal conductivity of nanofluids," Journal of Applied Physics, vol. 106, p. 094312, 2009.

[9] J. M. Wu and J. Zhao, "A review of nanofluid heat transfer and critical heat flux enhancement—Research gap to engineering application," Progress in Nuclear Energy, vol. 66, pp. 13-24, 2013.

[10] A. Sergis and Y. Hardalupas, "Anomalous heat transfer modes of nanofluids: a review based on statistical analysis," Nanoscale Research Letters, vol. 6, p. 391, May 19 2011.

[11] R. Hamilton and O. Crosser, "Thermal conductivity of heterogeneous two-component systems," Industrial & Engineering chemistry fundamentals, vol. 1, pp. 187-191, 1962.

[12] W. Yu and S. U. S. Choi, "The Role of Interfacial Layers in the Enhanced Thermal Conductivity of Nanofluids: A Renovated Maxwell Model," Journal of Nanoparticle Research, vol. 5, pp. 167-171, April 01 2003.

[13] B.-X. Wang, L.-P. Zhou, and X.-F. Peng, "A fractal model for predicting the effective thermal conductivity of liquid with suspension of nanoparticles," International Journal of Heat and Mass Transfer, vol. 46, pp. 2665-2672, 2003.

[14] T. G. Myers, M. M. MacDevette, and H. Ribera, "A time-dependent model to determine the thermal conductivity of a nanofluid," Journal of Nanoparticle Research, vol. 15, p. 1775, 2013.

[15] I. M. Mahbubul, R. Saidur, and M. A. Amalina, "Latest developments on the viscosity of nanofluids," International Journal of Heat and Mass Transfer, vol. 55, pp. 874-885, 2012.

[16] W. H. Azmi, K. V. Sharma, R. Mamat, G. Najafi, and M. S. Mohamad, "The enhancement of effective thermal conductivity and effective dynamic viscosity of nanofluids – A review," Renewable and Sustainable Energy Reviews, vol. 53, pp. 1046-1058, 2016.

[17] L. S. Sundar, K. V. Sharma, M. T. Naik, and M. K. Singh, "Empirical and theoretical correlations on viscosity of nanofluids: A review," Renewable and Sustainable Energy Reviews, vol. 25, pp. 670-686, 2013.

[18] K. Bashirnezhad, S. Bazri, M. R. Safaei, M. Goodarzi, M. Dahari, O. Mahian, et al., "Viscosity of nanofluids: A review of recent experimental studies," International Communications in Heat and Mass Transfer, vol. 73, pp. 114-123, 2016.

[19] Z. Haddad, E. Abu-Nada, H. F. Oztop, and A. Mataoui, "Natural convection in nanofluids: Are the thermophoresis and Brownian motion effects significant in nanofluid heat transfer enhancement?," International Journal of Thermal Sciences, vol. 57, pp. 152-162, 2012.

[20] S. M. Fotukian and M. Nasr Esfahany, "Experimental investigation of turbulent convective heat transfer of dilute γ-Al2O3/water nanofluid inside a circular tube," International Journal of Heat and Fluid Flow, vol. 31, pp. 606-612, 2010.

[21] Z. Haddad, H. F. Oztop, E. Abu-Nada, and A. Mataoui, "A review on natural convective heat transfer of nanofluids," Renewable and Sustainable Energy Reviews, vol. 16, pp. 5363-5378, 2012.

[22] E. B. Haghighi, A. T. Utomo, M. Ghanbarpour, A. I. T. Zavareh, E. Nowak, R. Khodabandeh, et al., "Combined effect of physical properties and convective heat transfer coefficient of nanofluids on their cooling efficiency," International Communications in Heat and Mass Transfer, vol. 68, pp. 32-42, 2015.

[23] T. G. Myers, H. Ribera, and V. Cregan, "Does mathematics contribute to the nanofluid debate?," International Journal of Heat and Mass Transfer, vol. 111, pp. 279-288, 2017.

[24] W. Yu, D. M. France, J. L. Routbort, and S. U. S. Choi, "Review and Comparison of Nanofluid Thermal Conductivity and Heat Transfer Enhancements," Heat Transfer Engineering, vol. 29, pp. 432-460, 2008.

[25] A. A. Abbasian Arani and J. Amani, "Experimental investigation of diameter effect on heat transfer performance and pressure drop of TiO2–water nanofluid," Experimental Thermal and Fluid Science, vol. 44, pp. 520-533, 2013.

[26] B. C. Pak and Y. I. Cho, "Hydrodynamic and heat transfer study of dispersed fluids with submicron metallic oxide particles," Experimental Heat Transfer, vol. 11, pp. 151-170, 1998.

[27] M. M. Heyhat, F. Kowsary, A. M. Rashidi, S. Alem Varzane Esfehani, and A. Amrollahi, "Experimental investigation of turbulent flow and convective heat transfer characteristics of alumina water nanofluids in fully developed flow regime," International Communications in Heat and Mass Transfer, vol. 39, pp. 1272-1278, 2012.

[28] R. Mondragón, C. Segarra, R. Martínez-Cuenca, J. E. Juliá, and J. C. Jarque, "Experimental characterization and modeling of thermophysical properties of nanofluids at high temperature conditions for heat transfer applications," Powder Technology, vol. 249, pp. 516-529, 2013.

[29] K. Khanafer and K. Vafai, "A critical synthesis of thermophysical characteristics of nanofluids," International Journal of Heat and Mass Transfer, vol. 54, pp. 4410-4428, 2011.

[30] A. T. Utomo, H. Poth, P. T. Robbins, and A. W. Pacek, "Experimental and theoretical studies of thermal conductivity, viscosity and heat transfer coefficient of titania and alumina nanofluids," International Journal of Heat and Mass Transfer, vol. 55, pp. 7772-7781, 2012.

[31] W. Williams, J. Buongiorno, and L.-W. Hu, "Experimental Investigation of Turbulent Convective Heat Transfer and Pressure Loss of Alumina/Water and Zirconia/Water Nanoparticle Colloids (Nanofluids) in Horizontal Tubes," Journal of Heat Transfer, vol. 130, pp. 042412-042412-7, 2008.

[32]   W. Duangthongsuk and S. Wongwises, "An experimental study on the heat transfer performance and pressure drop of TiO_2-water nanofluids flowing under a turbulent flow regime," International Journal of Heat and Mass Transfer, vol. 53, pp. 334-344, 2010.

[33]   M. M. MacDevette, T. G. Myers, and B. Wetton, "Boundary layer analysis and heat transfer of a nanofluid," Microfluidics and Nanofluidics, vol. 17, pp. 401-412, August 01 2014.

[34]   A. T. Utomo, E. B. Haghighi, A. I. T. Zavareh, M. Ghanbarpourgeravi, H. Poth, R. Khodabandeh, et al., "The effect of nanoparticles on laminar heat transfer in a horizontal tube," International Journal of Heat and Mass Transfer, vol. 69, pp. 77-91, 2014.

[35]   A. R. Sajadi and M. H. Kazemi, "Investigation of turbulent convective heat transfer and pressure drop of TiO_2/water nanofluid in circular tube," International Communications in Heat and Mass Transfer, vol. 38, pp. 1474-1478, 2011.

[36]   F. Incropera, "Fundamentals of heat and mass transfer. 6th ed2007, Hoboken," ed: NJ: John Wiley. xxv, 2007.

[37]   F. S. Alkasmoul, "Characterisation of the Properties and Performance of Nanofluid Coolants with Analysis of Their Feasibility for Datacentre Cooling," PhD Thesis, University of Leeds, 2015.

[38]   H. E. Patel, T. Sundararajan, and S. K. Das, "An experimental investigation into the thermal conductivity enhancement in oxide and metallic nanofluids," Journal of Nanoparticle Research, vol. 12, pp. 1015-1031, March 01 2010.

[39]   Sahin, B., et al., Experimental investigation of heat transfer and pressure drop characteristics of Al2O3–water nanofluid. Experimental Thermal and Fluid Science, 2013. 50(0): p. 21-28.

Tables

Table 1: Nanoparticles properties and sizes used. For comparison, the thermal conductivity of water at 20°C is 0.6 W/mK.

Nanoparticle type	Density (ρ_p) (kg/m^3)	Thermal conductivity (k_p) (W/m.K)	Specific heat capacity ($C_{p,p}$) (J/kg.K)	Nanoparticle size (nm)
Al_2O_3 Heyhat et al.[27]	3900	42.3	880	50
TiO_2 Sajadi & Kazemi et al. [35]	4170	11.8	711	45
CuO Patel et al. [38]	6310	18.0	549	30

Table 2: Comparison between thermal conductivity [W/mK] predictions for Al_2O_3-water nanofluids.

Ø Al_2O_3	Maxwell	Myers et al. [14]	Yu & Choi [12]
0.005	0.62111	0.61889	0.63036
0.009	0.62590	0.63579	0.64228
0.018	0.64605	0.65870	0.65700
0.027	0.66555	0.69319	0.68602
0.036	0.68377	0.71747	0.70672

Figures
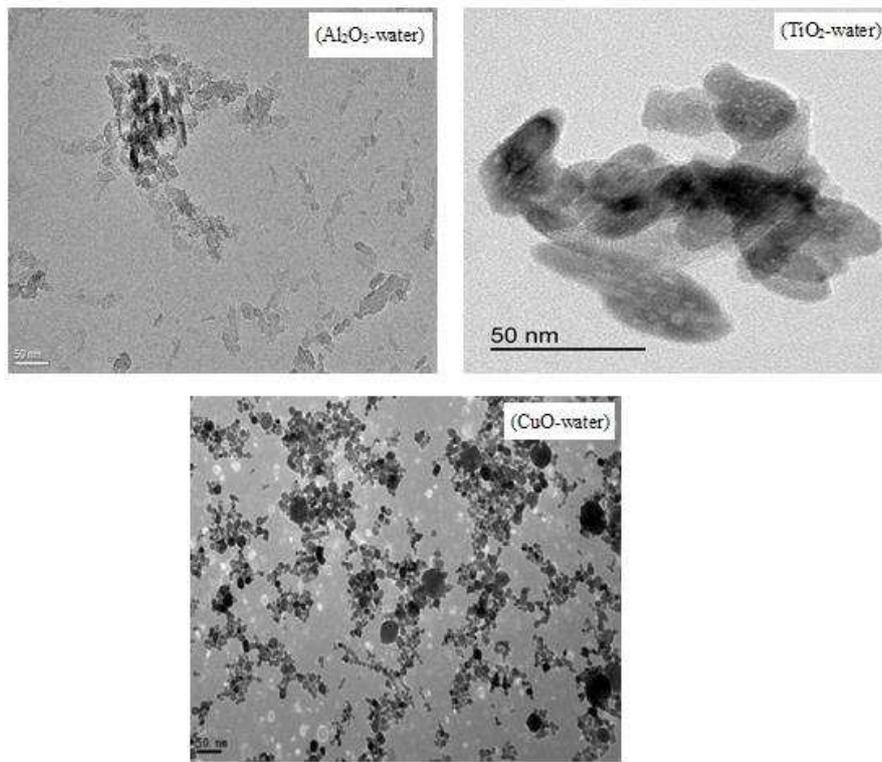
Figure 1: TEM images showing the shape and diameter of the Al$_2$O$_3$, TiO$_2$ and CuO nanoparticles.
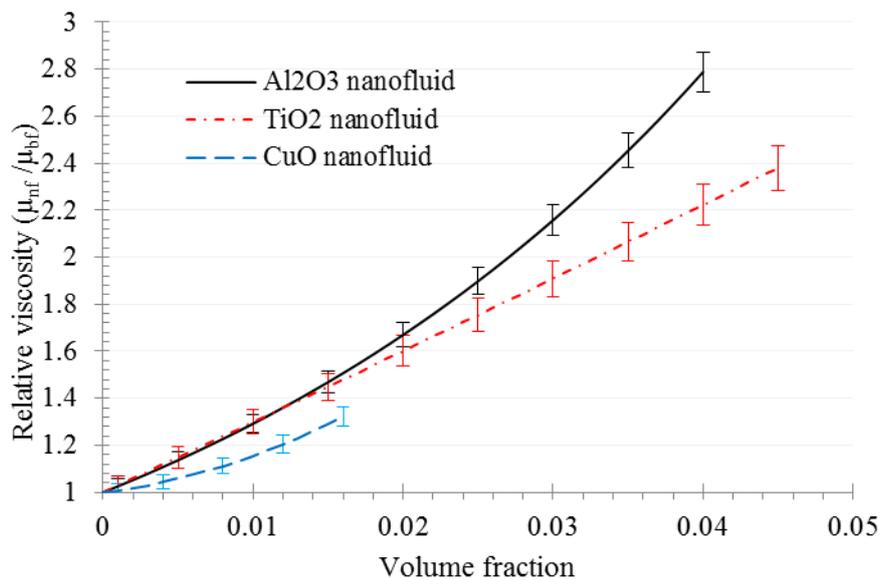
Figure 2: Relative viscosity measured for developed equations of Al$_2$O$_3$, TiO$_2$ and CuO nanofluids.
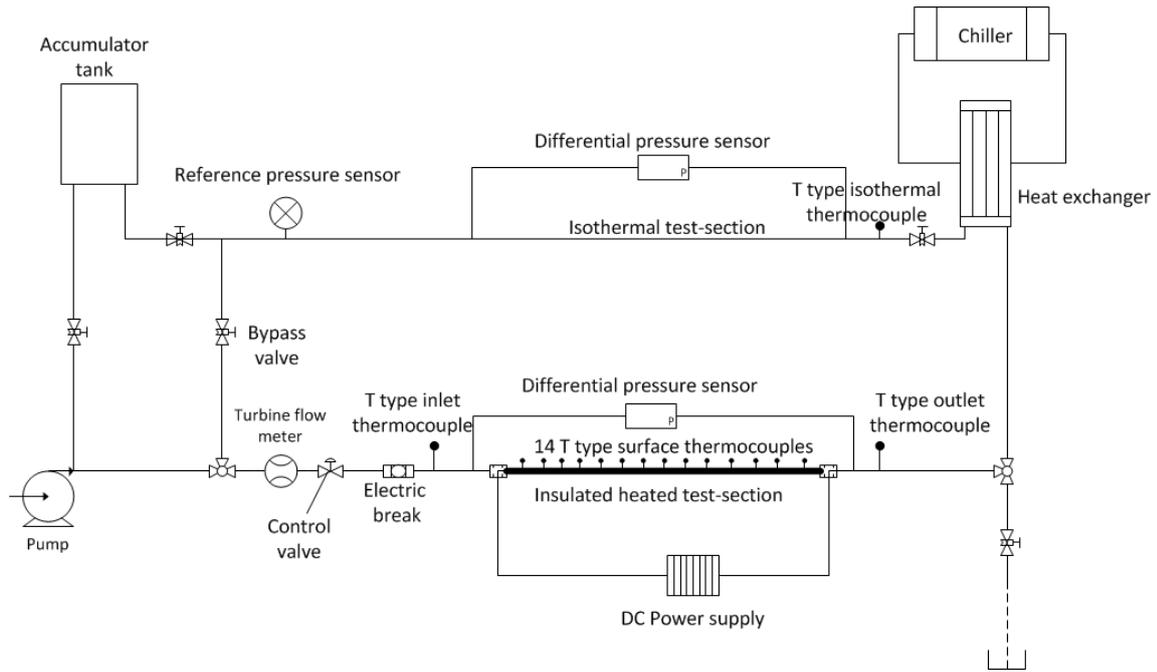
Figure 3: Schematic of the experimental loop setup.
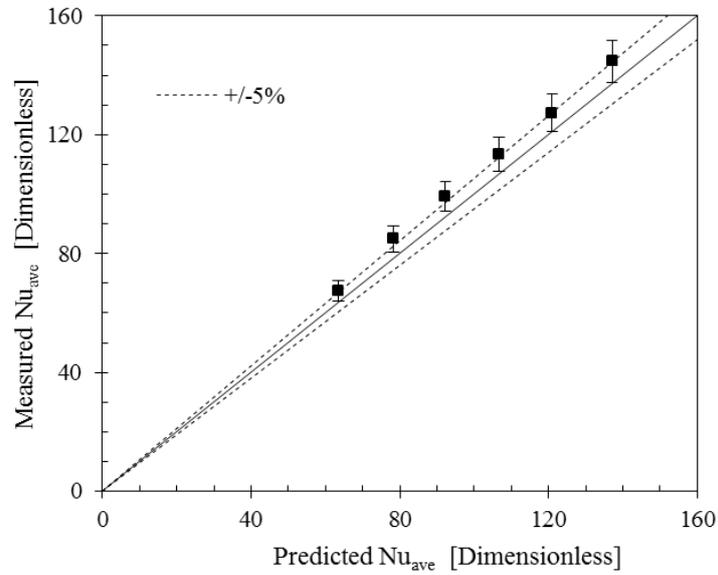
Figure 4: Comparison between the measured and the predicted (by Gnielinski's correlation) average Nusselt number for water tests.
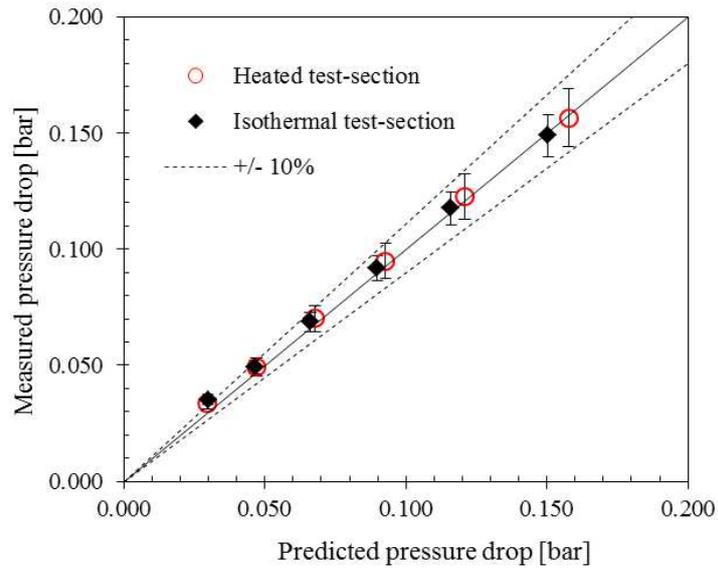
Figure 5: Water pressure drop comparison-test the heated and isothermal test sections.
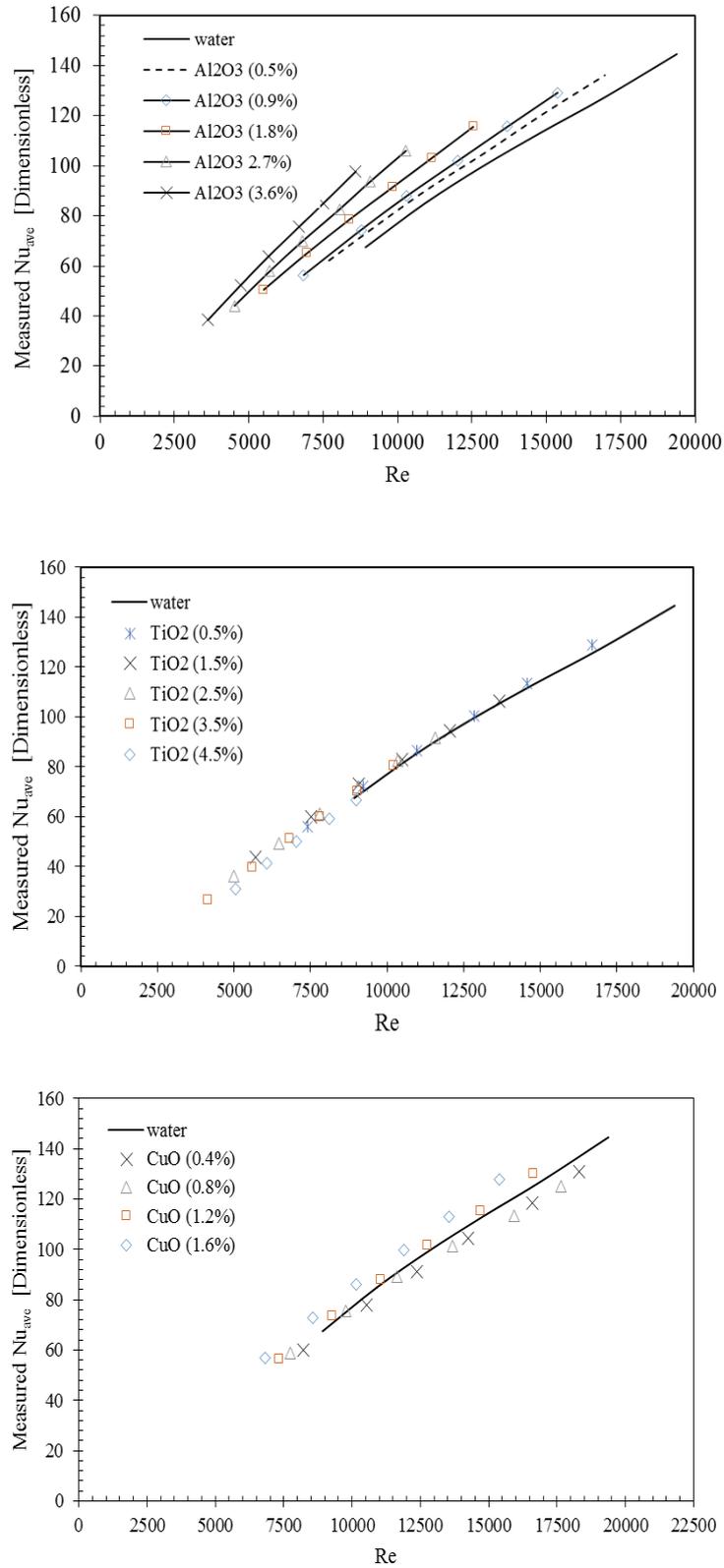
Figure 6: Average Nusselt number vs. Reynolds number for water and for Al_2O_3-, TiO_2-, and CuO-water nanofluids.
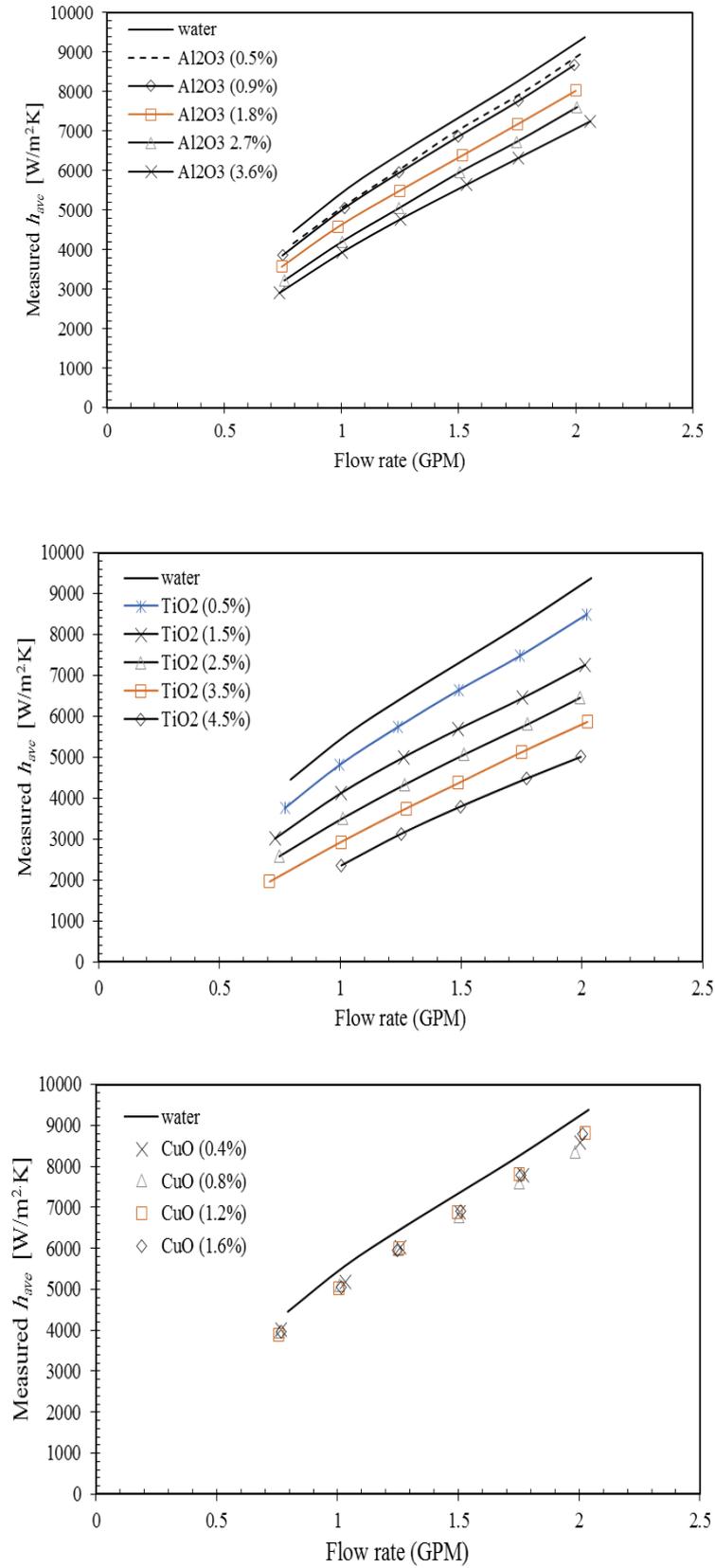
Figure 7: Average heat transfer coefficient vs. volumetric flow rate for water and for Al_2O_3-, TiO_2-, and CuO-water nanofluids.
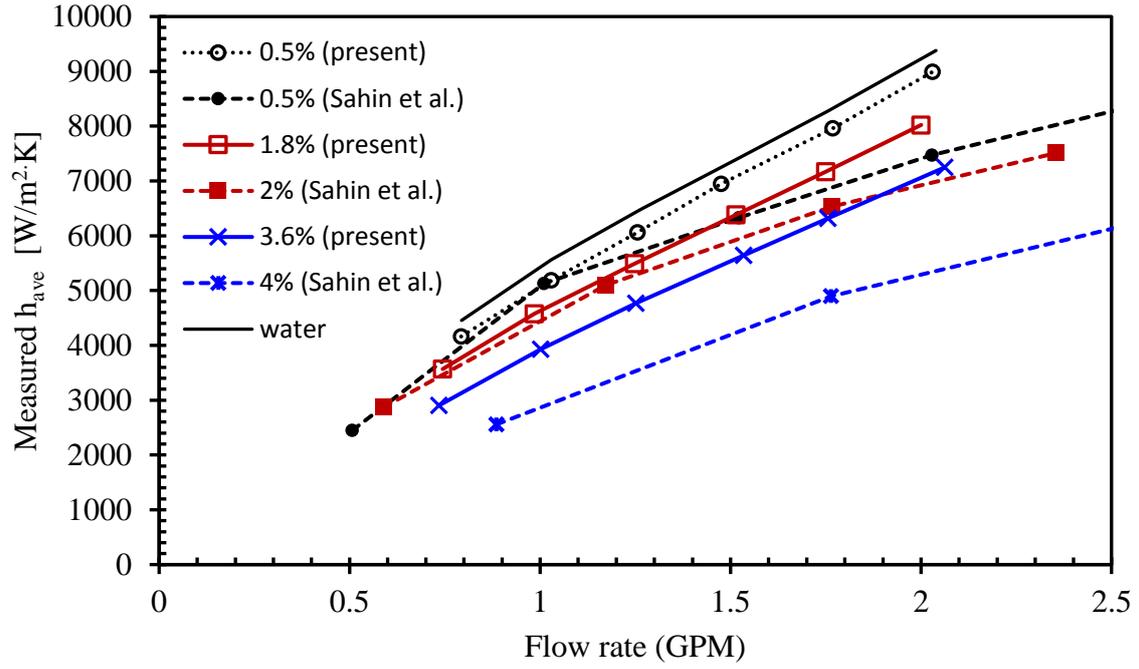
Figure 8: Average heat transfer coefficient for Al$_2$O$_3$-water nanofluids measured in the present study, compared with the results of Sahin et al. [39]. The percentages in the legend give the volume fraction.
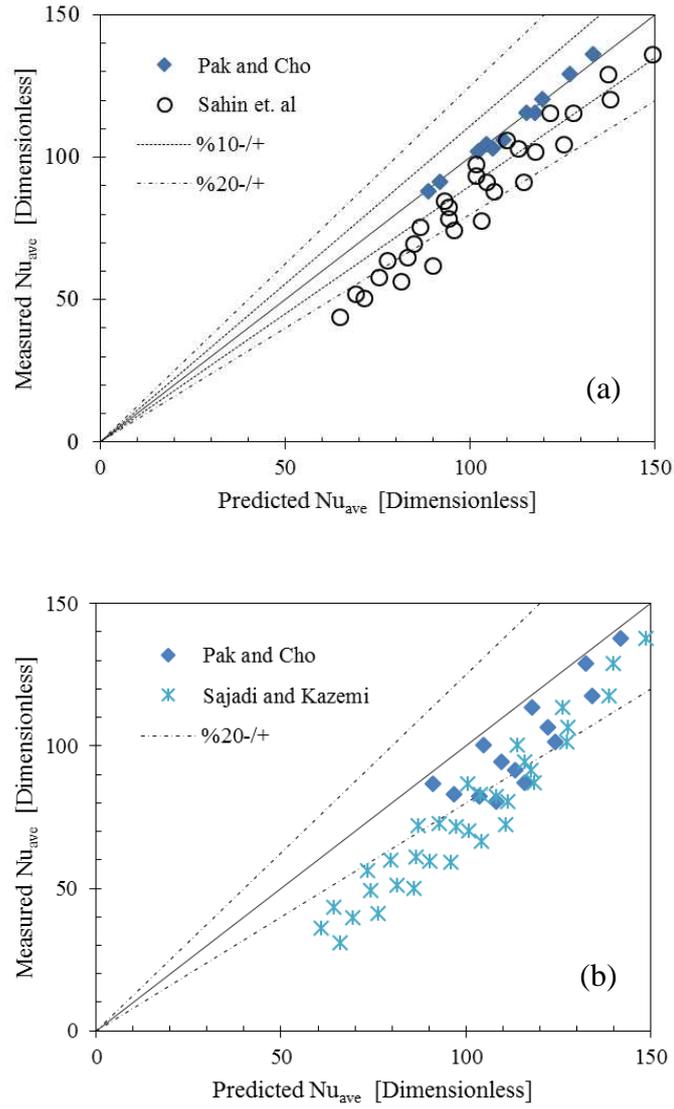
Figure 9: Comparison of the average Nusselt number measured in the present study with predictions from correlations (13)-(15) using corresponding nanofluid properties and conditions for (a) Al$_2$O$_3$-water and (b) TiO$_2$-water nanofluids.
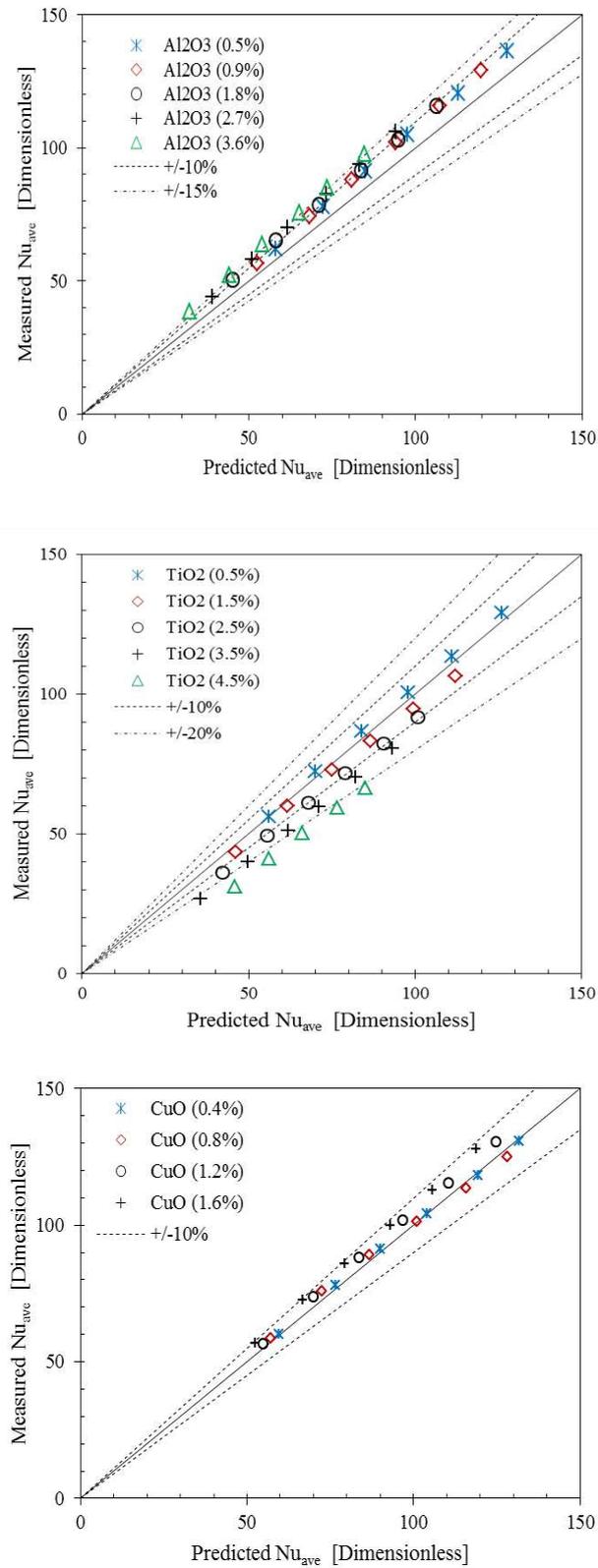
Figure 10: Comparison of the measured results and the Gnielinski correlation predicted average Nusselt numbers for Al_2O_3, TiO_2 and CuO-water nanofluids.
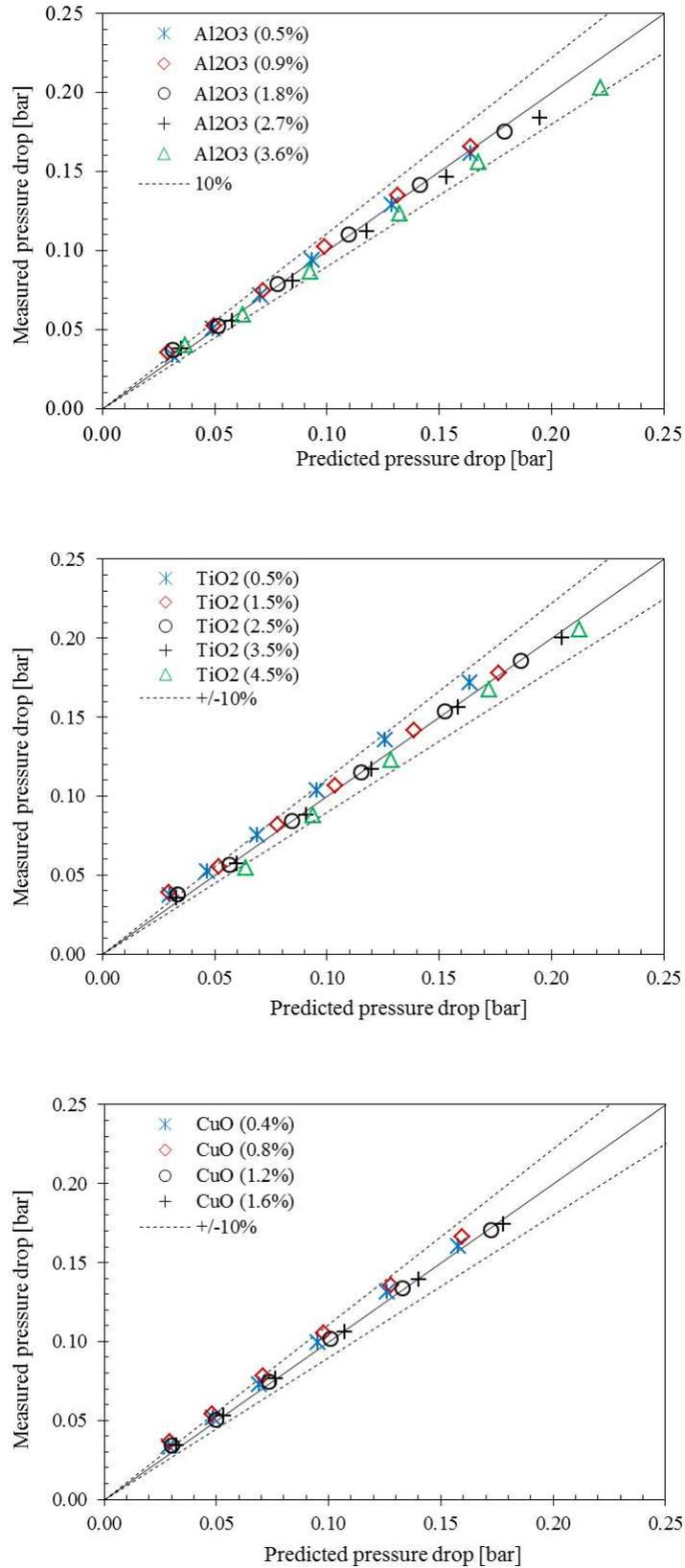
Figure 11: The measured pressure drop of heated section comparing to predicted pressure drop using Eq. (12) for Al₂O₃, TiO₂ and CuO water nanofluids.
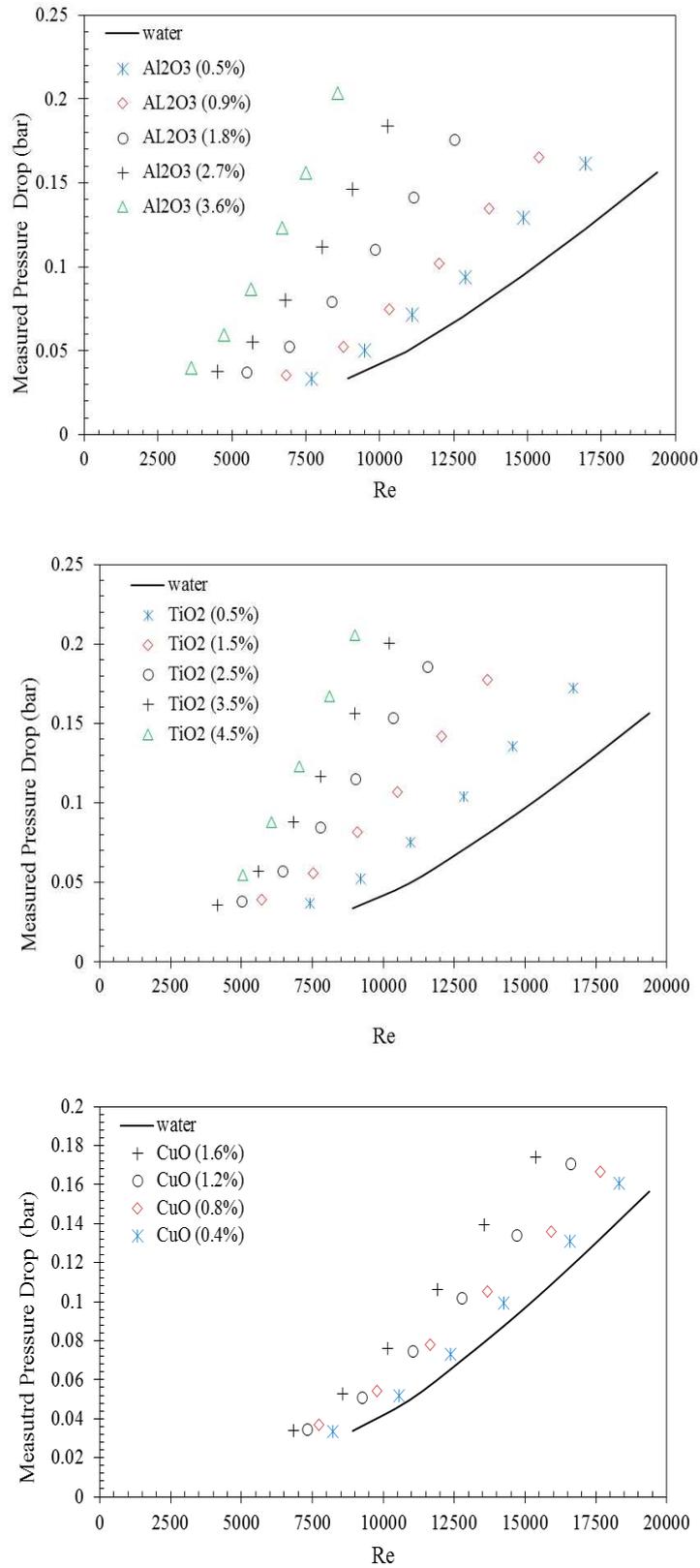
Figure 12: The measured pressure drop over the heated section versus Reynolds number for Al_2O_3, TiO_2 and CuO water nanofluids.
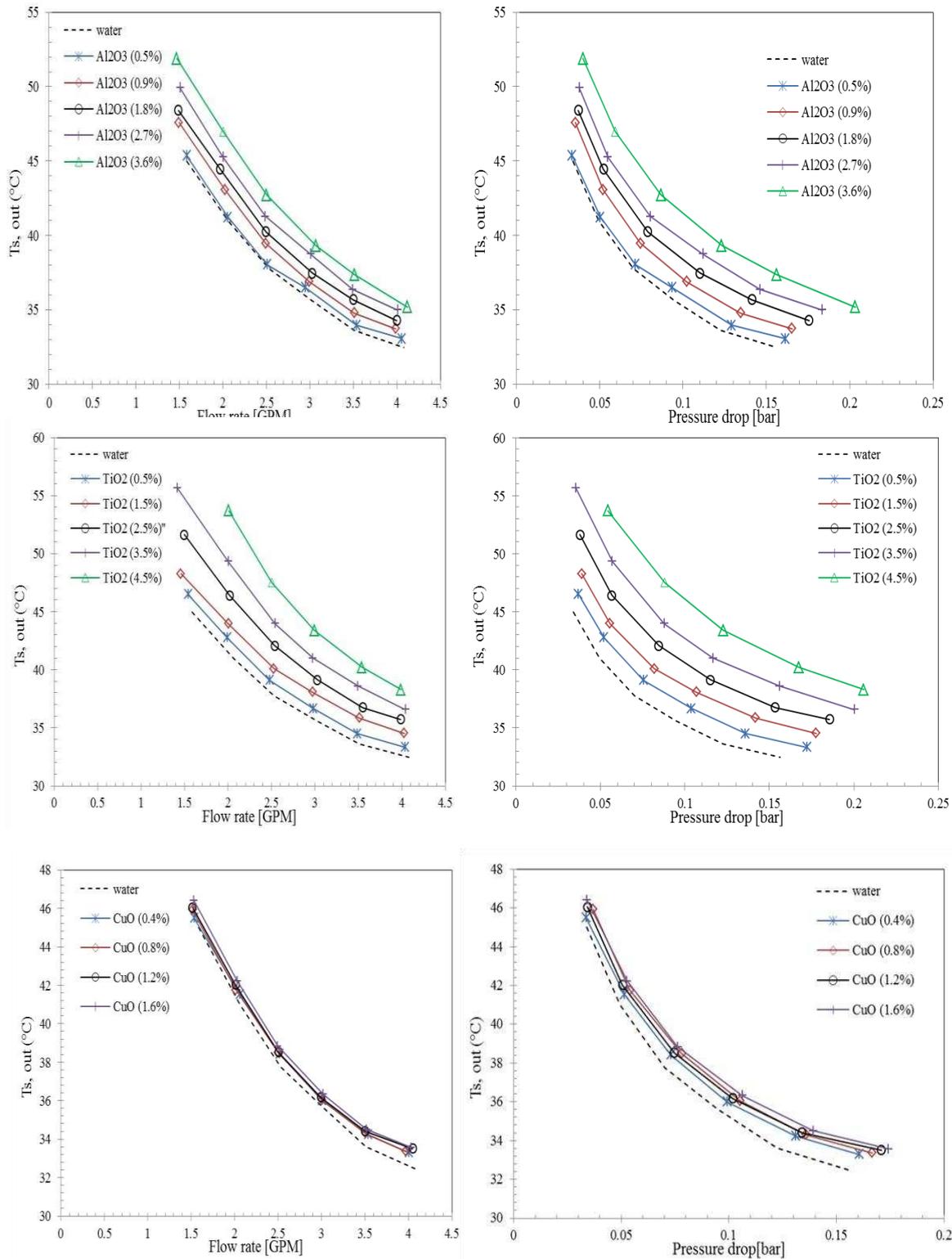
Figure 13: Outside surface temperatures of the test section as a function of flow rate and pressure drop for different concentrations of the three nanofluids considered. In each plot, the corresponding performance of the distilled water base fluid is included as the dashed lines.